IL NUOVO CIMENTO Vol. 34 C, N. 4 Luglio-Agosto 2011
DOI 10.1393/ncc/i2011-10933-7

Colloquia: Channeling 2010

Influence of crystals mosaicity on observed characteristics of X-ray emission along the propagation velocity of fast electrons in thick tungsten crystals

D. A. Baklanov, T. G. Duong, S. A. Laktionova, R. A. Shatokhin, I. E. Vnukov(*) and Yu. V. Zhandarmov

Belgorod State University - 14 Studencheskaya Str., 308007 Belgorod, Russia

(ricevuto il 22 Dicembre 2010; pubblicato online il 22 Agosto 2011)

Summary. — The results of a set of experiments on X-ray emission yield of $\omega \sim \gamma\omega_p$ energy, generated by 500 MeV energy electrons in oriented tungsten single crystals are presented. The experiments were performed at Tomsk synchrotron using crystal grating spectrometers based on mosaic crystals of pyrolytic graphite. It is shown that the measurement results are caused by the competition of two mechanisms: parametric X-ray emission along the particle velocity and bremsstrahlung diffraction in mosaic crystals of $a\alpha$ group. A method for determining the characteristic bulk dimensions in mosaic crystals of aα group is suggested.

PACS 61.05.C- – X-ray diffraction and scattering.
PACS 41.60.-m – Radiation by moving charges.
PACS 61.50.-f – Structure of bulk crystals.

1. – Introduction

Diffraction of the Coulomb field of a fast charged particle propagating in a crystal gives rise to parametric X-ray radiation (PXR) [1,2]. The theory predicts the existence of PXR reflections propagating both along the direction of Bragg scattering and at a small angle along the emitting particle velocity. However, while for the first of the observed reflections, studied in detail theoretically and experimentally, there is good coincidence between the experiment and the theory (see, for example, [3, 4] and references therein), PXR at small angles along the velocity of a particle, or as it is sometimes called the forward PXR, discovered recently in the experiments with tungsten crystal [5, 6] and silicon [7] does not yet have an adequate theoretical description.

The main difficulty in comparing the measurement results of forward PXR with the theory by contrast to the traditional PXR is that, when PXR emits at high angles to

(*) E-mail: vnukov@bsu.edu.ru

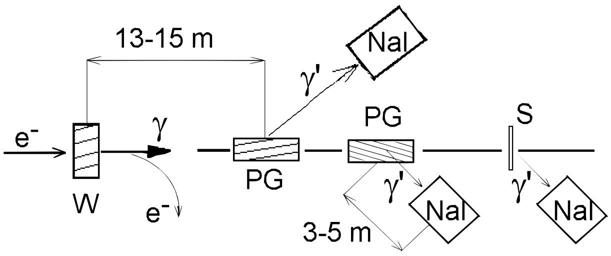

Fig. 1. – Experiment scheme. W—tungsten crystal; PG—crystals of pyrolytic graphite; NaI—NaI(Tl) spectrometers; S—converter.

the motion direction of the particle beam it can be relatively easily separated from background bremsstrahlung and measured by conventional X-ray detectors. The transition radiation and bremsstrahlung propagate in the same direction as that of a forward PXR, therefore the selection of this PXR branch became possible only by using crystal grating spectrometers. The efficiency of such devices essentially depends on the spectral and angular distribution of registered radiation, which makes the direct comparison of measurement results with the calculation difficult because the calculation must take into account the actual characteristics of the measuring equipment. An additional problem is that the photons of bremsstrahlung and transition radiation can also diffract in the crystal, where forward PXR was born, that complicates the interpretation of the results. Imperfection of the crystal structure can also affect the characteristics of the detected radiation. Basing on the above mentioned, it is important and relevant to describe the influence of experimental conditions and the contribution of the diffraction of real photons on the radiation yield in experiments on the forward PXR, in particular, in [5, 6].

2. – Experiments and measurements results

The scheme of the experiment [5] is shown in fig. 1. Electrons accelerated to final energy $E_0 = 500\,\mathrm{MeV}$ were incident on a single-crystal target placed in a goniometer. The radiation under study propagated through a collimator, "purified" by a magnet and was directed to an experimental hall, where the detecting equipment was installed. The crystal was oriented with respect to the electron beam direction according to the readings of a NaI (Tl) detector, in the Compton mounting, which detected photons upon channeling and bremsstrahlung with energy $\omega > 0.5\,\mathrm{MeV}$ scattered in the converter. The parameters of the electron beam, and experimental instruments and the method of orientation are considered in [8, 9].

To detect the radiation with fixed energy, two crystal grating spectrometers based on mosaic crystals of pyrolytic graphite with dimensions $2.5 \times 6.5 \times 22.5\,\mathrm{mm}^3$ and $3.5 \times 5.5 \times 20\,\mathrm{mm}^3$ mounted in goniometers at a distance of 13–15 m from the tungsten crystal, where the studied radiation was generated, were used. Distribution of mosaicity of the graphite crystals was determined during the experiment [10].

Under these conditions the energy resolution of spectrometers depends weakly on crystals mosaicity, but is determined by their angular aperture ($\Delta\theta_x \sim \pm 0.1\,\mathrm{mrad}$, $\Delta\theta_y = \pm 0.6\,\mathrm{mrad}$) and the collimation angle of the diffracted radiation $\Theta_x = 0.4$–$0.7\,\mathrm{mrad}$. In the work [11] on the basis of further development of the approach [10] a new method for calculating the efficiency of the spectrometers using the method of statistical simulation is

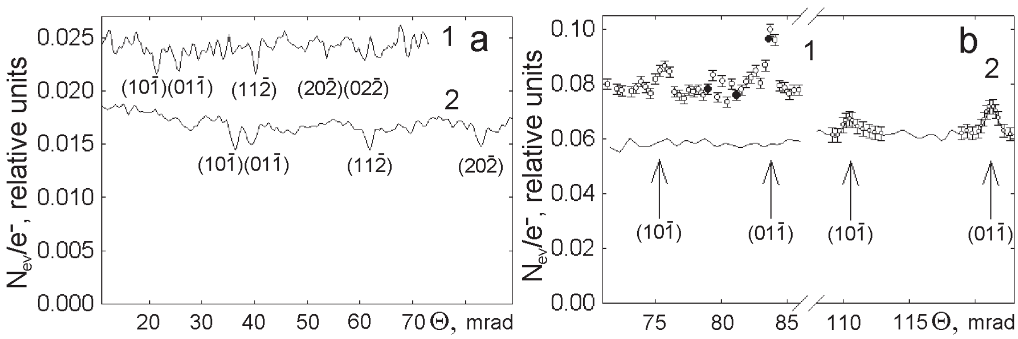

Fig. 2. – Orientation dependences of the X-ray radiation yield. a) $1: \omega = 95\,\text{keV}$; $2: \omega = 67\,\text{keV}$; b) 1: $\omega = 40\,\text{keV}$; $2: \omega = 28.3\,\text{keV}$.

suggested and implemented. During the matching of calculation and experiment results (see next section) the spectral distributions of the spectrometers efficiency, obtained using this technique, were used.

Measurements were performed for a tungsten single crystal of size $8.5 \times 0.41\,\text{mm}^3$, with the orientation of $\langle 111 \rangle$, and the surface mosaic structure $\sigma \leq 0.2\,\text{mrad}$. The crystal was mounted in the goniometer so that the plane $(11\bar{2})$ was almost vertical. This allowed to study the dynamic effects in radiation both for $(11\bar{2})$, and two planes (110), turned by 30° with respect to this plane. The measurements of orientation dependence (OD) of the yield of scattering radiation photons in the case of plane channeling [5] showed that the plane $(11\bar{2})$ is turned by the angle $\beta = 3.5^\circ \pm 0.2^\circ$ with respect to the vertical plane. Therefore, dynamic effects in radiation were observed for each of the crystal planes and fixed energy of photons for different orientation angles of the crystal.

In accordance with [12] a natural boundary manifestation of forward PXR is the photon energy $\omega = \gamma\omega_p \sim 80\,\text{keV}$, where γ is the Lorentz factor, and ω_p is the plasma frequency of the medium. Therefore, measurements were performed for photon energies $\omega = 96\,\text{keV} > \gamma\omega_p$, and three photon energies below this limit: 67 keV, 40 keV and 28.3 keV.

The measurements showed that for photon energies 96 keV and 67 keV no forward PXR peaks were observed. The presence of the crystal structure manifested in the decrease in the number of photons detected by spectrometers when the Bragg energy for the given orientation of the tungsten crystal coincided with the photon energy on which the spectrometer was tuned (see fig. 2a). The positions of minima in the ODs correspond to the kinematic conditions for diffraction of photons directed along the axis of the experimental setup, with an error not worse than 1%. For example, for $\omega = 67\,\text{keV}$ the calculated positions of minima for the reflections $(10\bar{1})$, $(01\bar{1})$ and $(11\bar{2})$ are 46.6 mrad 49.9 mrad and 72.2 mrad. Whereas the measured values are 46.3 mrad, 49.5 mrad and 71.9 mrad. In other words, the presence of dips in the hard photons yield is caused by bremsstrahlung diffraction inside the crystal. The depth of the minima changed from 15–18% for $\omega = 67\,\text{keV}$, up to $\sim 10\%$ for $\omega = 96\,\text{keV}$. The typical value of the full width of the minimum is $\Delta\Theta \sim 1.5$–$2.5\,\text{mrad}$.

Forward PXR was recorded only for photon energies $\omega = 40\,\text{keV}$ and $\omega = 28.3\,\text{keV}$ for which the maxima were observed, whose position, as minima for hard photons, agrees with Bragg's law (see fig. 2b). The position and shape of the maxima were reliably reproduced in the repeated measurements. Later the peaks for the $\omega = 40\,\text{keV} < \gamma\omega_p$ for the same tungsten crystal were obtained in the experiment [6].

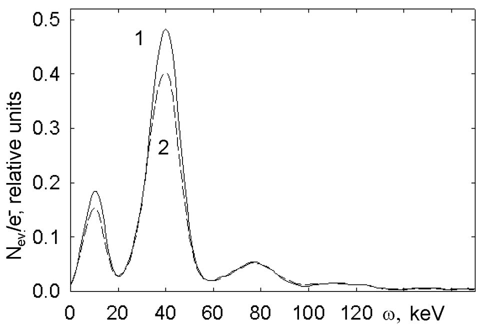

Fig. 3. – Spectra of diffracted radiation for $\omega_{\text{FPXR}} \sim 40\,\text{keV}$. Curve 1: $\Theta = 83.7\,\text{mrad}$; curve 2: $\Theta = 81.1\,\text{mrad}$ and $79.1\,\text{mrad}$.

To learn about the dependence of the emitted spectrum on the tungsten crystal orientation angle we performed measurements of the spectrum for several angles with the crystal grating spectrometer. In accordance with the method of ref. [10] we measured the diffracted radiation spectra for four reflection orders in the graphite crystal with a NaI(Tl) detector. Measurements were performed in the peak of the orientation dependence for the photon energy $\omega = 40\,\text{keV}$ ($\Theta = 83.7\,\text{mrad}$) and in the neighboring points ($\Theta = 81.1\,\text{mrad}$ and $79.1\,\text{mrad}$), curves 1 and 2 in fig. 3, respectively. The figure showed that the radiation intensity increases only for the first reflection order, *i.e.* for photon energies $\omega = 40\,\text{keV}$. For 2-4 reflection orders spectra are virtually identical. The large width of the peaks $\Delta\omega/\omega^{\text{exp}} \sim 25\%$ in comparison with $\Delta\omega/\omega^{\text{calc}} \sim 1\%$ is caused by the low resolution of the NaI(Tl) detector. The peak for $\omega \sim 12\,\text{keV}$ is caused by the emission of iodine CXR photons.

To determine the intensity for each reflection order Y_i with energy $\omega_i = i \cdot \omega_1$, where $\omega_1 = 40\,\text{keV}$ is the first-order reflection photon energy, the experimental spectra were "fitted" by the relationship

$$S_{\text{exp}}(k) = S_{\text{bg}}(k) + \sum_{i=0}^{n} \frac{Y_i}{\sqrt{2\pi}\sigma_i} \exp\left[-\frac{(k_i - k)^2}{2\sigma_i^2}\right].$$

Here S_{exp} is the measured spectrum, S_{bg} is the background spectrum, k is the channel number, i is the reflection order, k_i and σ_i are the peak position and resolution of the detector for i reflection order. As background spectrum the spectrum measured at the rotation of the graphite crystal at the angle $\Theta \sim \Theta_D/2$ in the opposite direction from the detector was used. The results of "fitting" are shown in table I. The errors are statistical and do not include the normalization error.

Table I.

Θ (mrad)	Y_1 (ev./e$^-$)	Y_2 (ev./e$^-$)	Y_3 (ev./e$^-$)	Y_4 (ev./e$^-$)
83.7	$(1.44 \pm 0.01) \cdot 10^{-9}$	$(1.71 \pm 0.02) \cdot 10^{-10}$	$(4.7 \pm 0.1) \cdot 10^{-11}$	$(2.7 \pm 0.4) \cdot 10^{-11}$
81.3	$(1.26 \pm 0.01) \cdot 10^{-9}$	$(1.82 \pm 0.02) \cdot 10^{-10}$	$(4.8 \pm 0.1) \cdot 10^{-11}$	$(2.7 \pm 0.2) \cdot 10^{-11}$
79.3	$(1.25 \pm 0.01) \cdot 10^{-9}$	$(1.82 \pm 0.02) \cdot 10^{-10}$	$(4.6 \pm 0.1) \cdot 10^{-11}$	$(2.6 \pm 0.2) \cdot 10^{-11}$

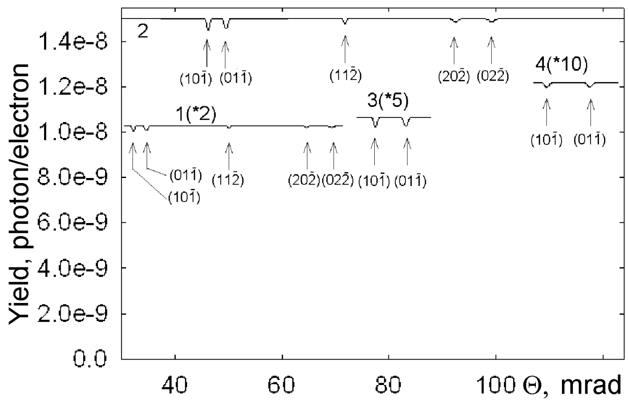

Fig. 4. – Calculated dependences of radiation yield. Curve 1: $\omega = 96\,\text{keV}$; curve 2: $\omega = 67\,\text{keV}$; curve 3: $\omega = 40\,\text{keV}$; curve 4: $\omega = 28.3\,\text{keV}$.

The table shows that the difference of the yields is observed only for the angle $\Theta = 83.7\,\text{mrad}$, which is close to the Bragg angle $\Theta_B = 83.14\,\text{mrad}$ for $\omega = 40\,\text{keV}$. The yield of photons with energies $\omega = 40\,\text{keV}$ at $\sim$ is 14% higher, and with energy 80 keV at $\sim$ is 6% lower than that outside the range of influence of diffraction effects, where photon yield does not depend on the crystal orientation.

3. – Analysis of the experimental results

The measurement of the photon yield for photon energies $\omega > \gamma\omega_p$, where the main mechanism for the formation of the observed OD is diffraction of bremsstrahlung, and for lower energies, where one can expect manifestations of both mechanisms [5, 13], allows to speak about the contribution of the bremsstrahlung diffraction for photon energies $\omega < \gamma\omega_p$ as well.

Figure 4 shows the calculated orientation dependences of the X-rays yield for the experimental conditions [5], taking into account the efficiency of the spectrometers and the contribution of the transition radiation from the outlet face of the crystal for a range of crystal disorientation angles 30–120 mrad and photon energies $\omega = 96\,\text{keV}$, $\omega = 67\,\text{keV}$, $\omega = 40\,\text{keV}$ and $\omega = 28.3\,\text{keV}$, in accordance with the dependence 1-4. The method of approximate estimation of the contribution of the diffraction suppression of radiation yield in perfect crystals is given in [14].

To confirm the calculation of the radiation yield table II shows comparison results of experimental and calculated radiation yields from a tungsten crystal for the experimental conditions [5] outside the range of influence of diffraction effects. The errors do not include the normalization error of the experimental data $\sim 15\%$. The results for the photon energies 28.3 keV, 40 keV, 67 keV and 96 keV are obtained directly from the measured OD of radiation yield, and for 80 keV and 120 keV from the spectra of the diffracted radiation (see fig. 3, curve 2 and table I). In the measured yields we considered the efficiency of the NaI(Tl) spectrometers, used in the experiment, calculated using the Monte Carlo method, the absorption of radiation in the outlet flange of the accelerator and in the air on the way from the accelerator to the detector. The calculation considers the efficiency of the spectrometers, the bremsstrahlung suppression due to the density effect [15] the radiation absorption in the crystal and the contribution of transition radiation from the outlet face of the target.

Table II.

ω (keV)	Y_{exp} (phot./elect.)	Y_{calc} (phot./elect.)	$Y_{\text{exp}}/Y_{\text{calc}}$
28.3	$(1.16 \pm 0.05) \cdot 10^{-9}$	$1.27 \cdot 10^{-9}$	0.96
40	$(2.0 \pm 0.1) \cdot 10^{-9}$	$2.13 \cdot 10^{-9}$	0.95
67	$(14.78 \pm 0.7) \cdot 10^{-9}$	$15.5 \cdot 10^{-9}$	0.95
80	$(0.40 \pm 0.02) \cdot 10^{-9}$	$0.36 \cdot 10^{-9}$	1.1
96	$(5.1 \pm 0.3) \cdot 10^{-9}$	$5.15 \cdot 10^{-9}$	0.99
120	$(3.6 \pm 0.4) \cdot 10^{-10}$	$3.47 \cdot 10^{-10}$	1.04

The figure shows that the depth of the dips in the calculated orientation dependences for planes (110) and photon energies 67 keV and 96 keV, respectively $\sim 2.5\%$ and $\sim 1.5\%$ is almost five times smaller than in the experimental ones $\sim 15\%$ and $\sim 10\%$. The width of the calculated dependences is roughly 1.5-2 times smaller than the experimental one (see previous section and fig. 2a). The position of confidently manifested dips coincides well with the calculation including the weaker reflecting planes (112) and (220). The experimental dips for these planes are 5-7 times deeper than the calculated ones.

It is known that mosaic crystals better reflect X-rays than perfect ones [16], that may explain the relatively deep dips in the measured OD. On the other hand, in the analyzed experiment the dynamic effect in fast electrons emission in crystals was first observed, that by default assumes the perfection of crystal structure. The way out of this dilemma is to take into account the fact that in mosaic crystals dynamic effects in the X-rays reflection can also occur [16]. For this purpose it is necessary that the dimensions of blocks with perfect structure are larger than the length of primary extinction ($\sim 2{-}3\,\mu$m). The particular bulks, rotated at a small angle $\Theta > \Delta\theta$ relative to the middle direction, increase the probability of reflection of photons with energy, at which the spectrometer is configured, that results in the increase of the dip depth and width.

To estimate the contribution of the diffraction losses effect to the detected radiation yield one can take the ratio of the absorption to the bulk average length. Based on the ratio between the experimental and calculated dip depths for photon energies $\omega = 67$ keV (~ 5.4) and the absorption length of photons with this energy $l_a \approx 183\,\mu$m the average dimension of blocks in the tungsten crystal used in the experiments of [5, 6] is $\sim 30\,\mu$m. Since $\sigma_m \approx 0.2$ mrad is comparable with the width of the Darwin table $\Delta\theta \sim 0.03$ mrad, then the effect of multiple reflections of the diffracted radiation should be observed, which causes the dip depth decrease. Therefore, the actual number of blocks, which caused the experimentally registered suppression of the bremsstrahlung yield, is higher and the average length of the blocks is, respectively, smaller. This is, in particular, proved by the fact that, for weak planes (112) and (220), for which the probability of multiple reflections is much lower because of the reduced $\Delta\theta$ and the increased l_{ex}, the relation of the amplitudes of the experimental and calculated dependences increases to ~ 8–10, which corresponds to the block length $\sim 20\,\mu$m.

To confirm the crucial contribution of mosaicity to the diffraction suppression of the bremsstrahlung yield we can refer to the fact that in the experiment [17], where the same experimental facilities and measurement techniques were used to study the dependence of the radiation yield on the orientation of a perfect silicon crystal, the dips in the yield of hard photons with energies $\omega > \gamma\omega_p$ were not observed at a essentially lower statistical error. Whereas in similar measurements for the tungsten crystal with a thickness of 1.7 mm and a surface mosaicity $\sigma \sim 0.5$ mrad [18] such dips were distinguished clearly.

The absence of a dip in the photons yield OD with $\omega = 40$ keV in the experiment [5] is caused by the forward PXR contribution, compensating the loss of radiation yield due to bremsstrahlung diffraction inside the crystal for the energy range $\omega < \gamma\omega_p$. Good agreement between the measured and calculated radiation yields for the photons energy $\omega = 40$ keV and 28.3 keV, outside the range of influence of diffraction effects allows to estimate forward PXR yield from the tungsten crystal for the conditions of this experiment. For the photon energy $\omega = 40$ keV, solid angle $\Delta\Omega = 2.02 \cdot 10^{-7}$ sr and energy capture of the spectrometer $\Delta\omega = 0.276$ keV (FWHM) the excess of the yield at the maximum of OD for the plane $(01\bar{1})\Delta Y_{\mathrm{exp}} = (0.58 \pm 0.1) \cdot 10^{-9}$ phot./elect. $\sim 28\%$ of the total bremsstrahlung and transition radiation yield outside the region of the influence of diffraction effects was detected. For the photon energy $\omega = 28.3$ keV, $\Delta\Omega = 1.94 \cdot 10^{-7}$ sr and $\Delta\omega = 0.172$ keV this value was $\Delta Y_{\mathrm{exp}} \sim 22\%$ of the incoherent substrate. A lower value of forward PXR contribution for this photon energy is caused by the large contribution of transition radiation from the crystal outlet face ($\sim 68\%$) compared with the measurements for $\omega = 40$ keV ($\sim 20\%$).

For the experimental conditions [5], the perfect crystal, the plane $(01\bar{1})$ and the photon energy $\omega = 40$ keV, the depth of the dip, caused by bremsstrahlung diffraction, in accordance with the calculation results must be $\sim 5\%$ of the substrate. For the length of the absorption $l_a \approx 48\,\mu$m and the average block size $l \sim 20\,\mu$m the suppression of bremsstrahlung yield of about 10% of the substrate should be observed due to the mosaic diffraction. Consequently, the observed OD for the photon energy $\omega = 40$ keV (see fig. 2b, curve 1) is the sum of the photon yield OD from forward PXR with the amplitude $Y_{\mathrm{exp}}^{\mathrm{FPXR}} \approx (0.8 \pm 0.1) \cdot 10^{-9}$ phot./elect. $\sim 40\%$ of the substrate and of OD due to the bremsstrahlung diffraction suppression in a mosaic crystal with the depth of $\sim 10\%$ of the total photon yield outside the range of influence of diffraction effects.

In the experiment [6], where the same tungsten crystal was used, for photon energy $\omega = 40$ keV the forward PXR yield is comparable with the resulting yield of the bremsstrahlung and the transition radiation. Basing on the data on the experiment geometry, given in the above cited work, we calculated the characteristics of the spectrometer for photons energy $\omega = 40$ keV by the method of [14] and obtained the following values of energy and angular captures of the spectrometer $\Delta\omega \approx 0.176$ keV and $\Delta\Omega \sim 1.16 \cdot 10^{-7}$ sr. Outside the range of influence of diffraction effects the estimated value of the photon yield from a tungsten crystal, detected by the spectrometer, coincides with the estimated value given in [6], with an error of $\sim 10\%$.

The increase in electron energy from 500 MeV to 855 MeV in the experiment [6] resulted in the suppression of the intensity of the bremsstrahlung due to density effect of Ter-Mikaelian [19] and the decrease of the relative fraction of the bremsstrahlung up to $\sim 40\%$. Because of the improved energy resolution the depth of calculated OD for a perfect crystal rose to $\sim 10\%$. Therefore, reducing the amplitude of the maximum, caused by the forward PXR, due to the diffraction suppression of the bremsstrahlung yield in the mosaic crystal with the characteristic length of the block $\sim 25\,\mu$m should not exceed 10% of the incoherent substrate.

The obtained results allows to offer a new way to evaluate the quality of thick crystals structure and characteristic size of bulks by the relation of the experimentally measured value of diffraction suppression with the calculated or measured one for a perfect crystal.

These measurements can be done on the medium-energy electron ($E_0 \sim 30\,\text{MeV}$). Basic requirements are: a goniometer with a rotation step of no more than 0.1 mrad and a sufficiently large basis, by which one could implement the method of isolating the radiation with fixed energy and resolution of $\Delta\omega/\omega \leq 0.5\%$ using a crystal grating spectrometer based on a perfect or mosaic crystal.

4. – Conclusion

The results of these studies can be briefly formulated as follows:

1) The measurement results of the X-ray yield in the experiments [5, 6] are caused by the competition between two mechanisms: forward PXR and bremsstrahlung diffraction in mosaic crystals of $a\alpha$ class.

2) Based on the comparison of the measured diffraction suppression of radiation emission with the calculated or measured one for a perfect crystal one can define the average size of the bulk along the motion direction of the electrons.

* * *

The authors thank the co-authors of [5, 18] for participation in the development and implementation of methods used in the research and the measurements. This work was partly supported by the Federal Program "Academic and Teaching Staff of Innovation Russia", the government contract 16.740.11.0147 dated 02.09.2010.

REFERENCES

[1] Garibian G. M. and Yang C., *Sov. Phys. JETP*, **34** (1972) 495.
[2] Baryshevsky V. G. and Feranchuk I. D., *Sov. Phys. JETP*, **34** (1972) 502.
[3] Baryshevsky V. G. and Dubovskaya I. Y., *Itogi Nauki Tekh., Puchki Zariazhennykh Chastic i Tverdoe Telo*, **4** (1991) 129 (in Russian).
[4] Brenzinger K.-H. *et al.*, *Z. Phys.*, **358** (1997) 107.
[5] Aleynik A. N. *et al.*, *JETP Lett.*, **80** (2004) 393.
[6] Backe H. *et al.*, *Proc. SPIE*, Vol. **6634**, 66340Z (arXiv:physics/0609151 v1 18 Sep 2006).
[7] Backe H. *et al.*, *Nucl. Instrum. Methods B*, **234** (2005) 130.
[8] Adishchev Yu. N. *et al.*, *Yad. Fiz.*, **35** (1982) 108.
[9] Kalinin B. N. *et al.*, *Instrum. Exp. Tech.*, **28** (1985) 533.
[10] Vnukov I. E. *et al.*, *Russ. Phys. J.*, **44** (2001) 315.
[11] Baklanov D. A., Duong T. G., Laktionova S. A., Zhandarmov Yu. V., Shatokhin R. A. and I. E. Vnukov, these proceedings.
[12] Kubankin A., Nasonov N., Sergienko V. and Vnukov I., *Nucl. Instrum. Methods B*, **201** (2003) 97.
[13] Likhachev V., Nasonov N., Tulinov A. and Zhukova P., *Vestn. Voronezhskogo Gosudarstvennogo Univ. Ser. Fiz. Mat.*, **2** (2005) 98.
[14] Baklanov D. A. *et al.*, *Vestn. Khark. Nat. Univ. Ser. Fiz.*, **763** (2007) 41 (in Russian).
[15] Kleyner V. P., Nasonov N. N. and Shlyahov N. A., *Ukr. Phys. J.*, **57** (1992) 48 (in Russian).
[16] James R., *Optical Principles of X-ray Diffraction* (G. Bell and Sons, London) 1958.
[17] Kalinin B. N. *et al.*, *Nucl. Instrum. Methods B*, **173** (2001) 253.
[18] Bogomazova E. *et al.*, *in V International Symposium "Radiation from Relativistic Electrons in Periodic Structures", Book of Abstracts* (2001).
[19] Ter-Mikaelian M. L., *High-Energy Electromagnetic Processes in Condensed Media* (Wiley-Interscience, New York) 1972.